Effect of Electrostatic Interactions between Glycosaminoglycans on the Shear Stiffness of Cartilage: A Molecular Model and Experiments

Moonsoo Jin* and Alan J. Grodzinsky

Continuum Electromechanics Group, Center for Biomedical Engineering, Department of Mechanical Engineering, Department of Electrical Engineering and Computer Science, Massachusetts Institute of Technology, Cambridge, Massachusetts 02139

Received April 16, 2001; Revised Manuscript Received August 13, 2001

ABSTRACT: This study focuses on the contribution of repulsive electrostatic interaction between glycosaminoglycan (GAG) molecules in cartilage to the shear properties of the tissue. We first measured the equilibrium and dynamic shear moduli of cylindrical disks of cartilage at varying ionic concentrations (0.01−1.0 M NaCl). We then used a molecular model of GAG electrostatic interactions that would occur during macroscopic shear deformation to predict the dependence of the shear properties of cartilage on the ionic strength of the bath. The molecular model of GAG interaction was based on approximating GAG segments as charged rods, i.e., the unit cell model and then changing the shape of the unit cell in a manner consistent with the macroscopic shear deformation. The Poisson−Boltzmann equation was incorporated into the unit cell model (PB unit cell) to predict physical phenomena such as the change in electrical potential and mobile ion distribution caused by macroscopic shear deformation and changes in bath ionic concentration. The nonlinear PB equation was solved numerically using finite element methods (FEM) within the unit cell. The electrostatic free energy was calculated from the numerically obtained electrical potential and the associated mobile ion distribution, and the electrical contribution to the equilibrium shear modulus was obtained using an energy method. Using physiologically relevant values for the GAG concentration and the nonelectrical contribution to the shear modulus (the two adjustable parameters of the model), the theory predicted the observed dependency of the equilibrium shear modulus on ionic concentration rather well. These results confirmed the validity of the proposed model of the GAG interactions under pure shear deformation and, accordingly, the important role of electrostatic interactions to the shear stiffness of cartilage extracellular matrix.

Introduction

Glycosaminoglycans (GAGs) are polymers of disaccharides that contain alternating sequences of glucuronic acid (GlcA) and either *N*-acetylglucosamine (GlcNAc) or *N*-acetylgalactosamine (GalNAc). The family of GAG molecules, including hyaluronic acid (HA), chondroitin sulfate (CS), keratan sulfate (KS), and heparan sulfate (HS),[1] plays an important role in the mechanical and transport properties of extracellular matrix (e.g., CS, HA)[2] and in cell surface ligand binding interactions (e.g., HS).[3] For example, chondroitin sulfate GAG (CS-GAG) contains on the average one negatively charged carboxylate and sulfate group per disaccharide which is completely ionized under physiological pH conditions. Therefore, the high negative charge density and associated electrical repulsion between CS-GAGs play an important role in electromechanical and physicochemical interaction within biological tissues such as cartilage.

The role of electrical repulsive interactions is particularly critical in articular cartilage, a tissue that covers the ends of bones in synovial joints, providing compressive and shear stiffness during the relative motion of opposing joint surfaces. The compressive resistance of cartilage is mainly due to highly charged CS-GAGs (Figure 1C) which are attached to a core protein, forming the proteoglycan called aggrecan (Figure 1B). Aggrecan molecules, in turn, bind noncovalently to long hyaluronic acid (HA) chains, forming supramolecular proteoglycan aggregates (Figure 1A) which are enmeshed within a resilient collagen network. At physiologic pH, the properties of the collagen fibrils do not change significantly with ionic strength in the range 0.01−1.0 M.[4,5] Therefore, the mechanical properties of cartilage can be modeled in terms of two distinct electrical and nonelectrical contributions. Electrical contributions to the mechanical properties of cartilage are mainly associated with the electrostatic repulsive forces between CS-GAGs. In contrast, nonelectrical contributions to cartilage properties are associated with the resilience of the electrically neutral collagen fibrils as well as the elastic forces due to the steric and entropic effects induced by volumetric deformation of GAG and other matrix macromolecules.

Often the definition of free energy provides a way to derive macroscopic constitutive material properties such as compressive and shear moduli.[6] Intermolecular interactions and intramolecular conformational changes have been explained by using the free energy function.[7] In cartilage, the electrostatic free energy is mainly associated with the charged GAG constituents and depends on the chemical environment (e.g., the pH and ionic concentration), temperature, and mechanical deformation, which can modulate the fixed charge density. However, the nonelectrical free energy depends on mechanical deformation, volume change, and temperature and not on the chemical environment such as ionic concentration and small pH changes around 7.0.

The Poisson−Boltzmann (PB) mean field theory has been used to model electrical properties of polyelectrolytes and colloidal systems containing charged macromolecules within electrolyte solutions. For example, the osmotic swelling pressure of proteoglycan solutions[8] has been modeled quantitatively using the PB equation. The GAG constituent has been modeled as a cylindrical rod with a surface charge, and the geometry of the sur-

* To whom correspondence should be addressed: Tel (617) 253-5892; Fax (617) 258-5239; E-mail msjin@mit.edu.

10.1021/ma0106604 CCC: $20.00
Published on Web 10/11/2001

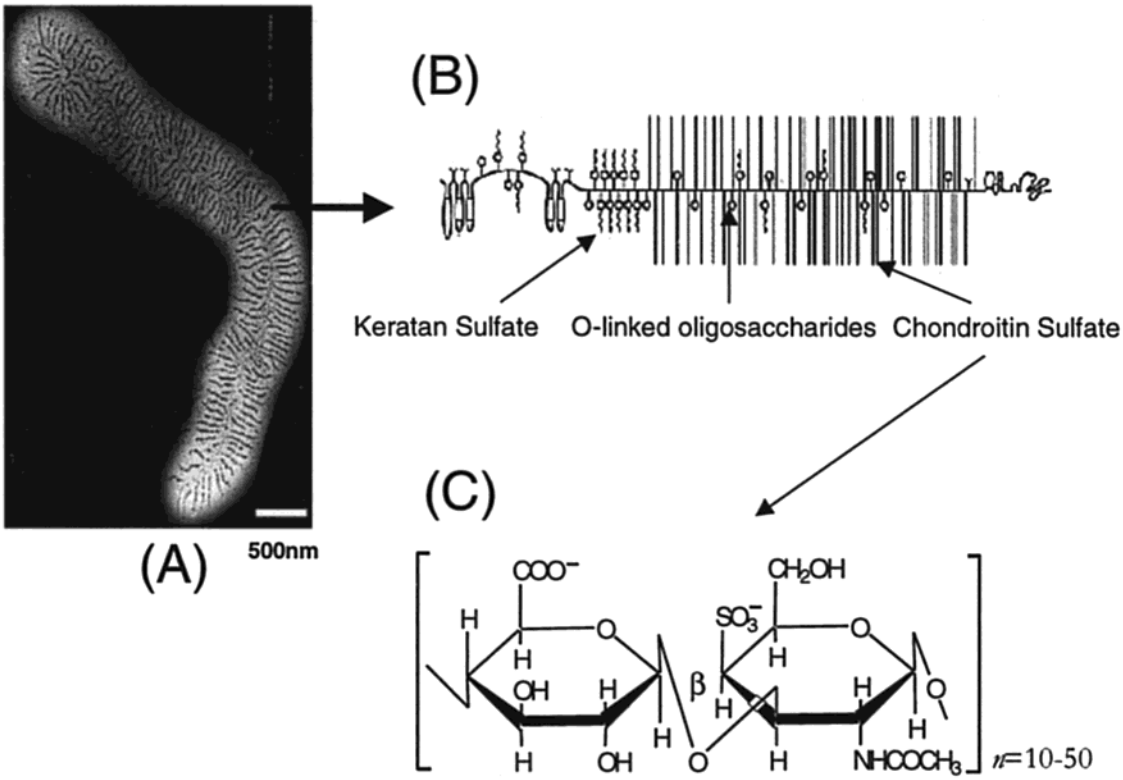

Figure 1. The cartilage supramolecular proteoglycan aggregate (A) consists of proteoglycan monomers called aggrecan (B) which are noncovalently attached to hyaluronic acid (HA) molecules. Aggrecan, in turn, consists of glycosaminoglycan chains covalently attached to a core protein (B). The chondroitin sulfate GAG chains (C) of aggrecan are mainly responsible for the compressive stiffness of cartilage through electrical repulsion interactions. On the average, CS-GAG disaccharides have one carboxylate and sulfate group which are negatively charged at physiologic pH. Parts A and B are adapted from the literature.[33,34]

rounding unit cell structure was based on experimental measurements.[9] Furthermore, the GAG unit cell model was extended to estimate the contribution of GAG electrostatic interactions to the compressive stiffness of cartilage.[9] In this study, we focused on the contribution of GAG electrostatic interaction in determining the shear stiffness of a material like cartilage. The role of GAGs in the shear properties of articular cartilage has been previously described as inflating the collagen network, causing a tensile prestress that enables the collagen−aggrecan matrix to resist shear deformation.[10−13] Previous studies showed that cartilage shear modulus changed significantly after extraction of aggrecan[11] and that increased ionic strength could decrease the shear modulus inferred from the measurement of compressive modulus at confined compression tests.[13] However, there has been little theoretical or experimental study of the possible mechanisms by which GAG electrostatic interactions may contribute directly to the tissue shear stiffness and the importance of this contribution compared to that of other nonelectrical interactions.

In this study, we first performed experiments to measure the equilibrium and dynamic shear stiffness of cartilage under torsional shear deformation at varying bath ionic concentrations. Experimental results showed a significant change in the measured shear modulus with changes in ionic strength between 0.01 and 1.0 M. We hypothesized that any dependence of the shear modulus with ionic strength comes from the GAG-associated electrical interactions, which are supported by means of the tissue's collagen network. However, using a macroscopic model of a polyelectrolyte system such as the Donnan model, the electrostatic free energy should be constant under torsional shear, since this deformation does not induce any volume change and therefore no change in fixed charge density. Therefore, it was hypothesized that rearrangement of GAG molecules at a microscopic scale could provide increased resistance to shear deformation and increased shear stiffness with decreasing salt concentration. Using a PB unit cell model of GAG electrostatic interactions under shear deformation, we calculated the change in the electrical contribution to the equilibrium shear modulus at each ionic concentration. To account for the nonlinearity of the PB equation and the geometry of the model, we used the finite element method to solve the electrical potential and mobile ion distribution. From this calculation, the electrical contribution to shear stress was obtained by differentiating the electrostatic free energy with respect to the shear deformation. Finally, the electrical contribution to the equilibrium shear stiffness was calculated from the slope of stress vs strain, and the resulting shear stiffness was compared to the experimental measurements.

Experimental Section

Cartilage disks (9.65 mm diameter by 1 mm thick) were obtained under sterile conditions from the femoropatellar groove of 1−2 week old bovine calves as previously described[14] and maintained in living organ culture for 1−3 days until testing (DMEM + 10% fetal bovine serum). Prior to measurement, cartilage disks were equilibrated in 0.15 M NaCl solution up to 30 min. The disks were then placed in the base of a Plexiglas chamber filled with a 0.15 M NaCl bathing solution. The base chamber was placed in the bottom grip of a specially designed biaxial rheometer capable of applying axial deformations as small as 1 μm and sinusoidal rotations as small as 0.001°.[14] An upper aluminum platen fixed to a

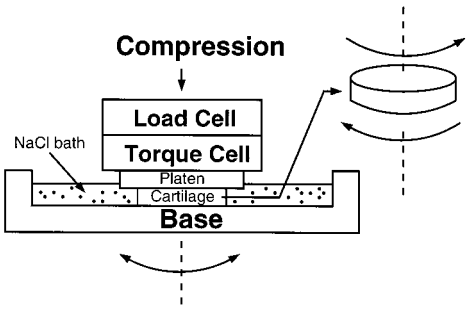

Figure 2. Cartilage disks (9.65 mm diameter by 1 mm thickness) were placed in the center of the Plexiglas base chamber filled with NaCl solution at room temperature. An upper aluminum platen attached to a torque cell was used to apply a 10% compressive offset strain to the specimen. Fine grit sandpaper glued to the base and upper platen made contact with top and bottom cartilage surfaces to prevent slippage between the specimen and apparatus. Equilibrium and dynamic shear modulus were measured at NaCl bath concentrations varied sequentially from 0.15, 0.05, 0.01, 0.5, to 1.0 M NaCl.

torque cell (Figure 2) was used to apply a 10% compressive offset strain to the specimen. After mechanical and chemical equilibration was achieved in this state (~15 min), torsional deformation was applied by rotating the bottom chamber with respect to the top platen, and the resulting torque was measured by the torque cell. From the measured torque and applied torsional deformation, the shear strain, γ, and shear stress, τ, were calculated as $\gamma(r) = \theta r/h$ and $\tau(r) = Tr/I$, where θ is the angular deformation, r is the radial distance, h is the height of the disk, T is the measured torque, and I is the polar moment of inertia ($I = \pi R^4/2$, R is the radius of the disk). Fine grit sandpaper glued to the base and upper platen was used to prevent slippage between the specimen and these platens. For measurement of the equilibrium modulus, a ramp-and-hold shear strain of 1.5% was applied, resulting in an initial increase and subsequent relaxation of the shear stress (Figure 3A). This sequence was repeated four times, and the slope of the relaxed equilibrium stress and strain was used to compute the equilibrium modulus. After returning the specimen to 0% shear strain, a 0.8% amplitude sinusoidal shear strain was applied at 0.5 Hz (Figure 3B). The magnitude of the dynamic shear modulus was calculated as $G = |\tau|/|\gamma|$. The shear stress and strain signals were continuously recorded by a computer, and a discrete Fourier transform (DFT) was implemented to calculate the amplitudes of the fundamental and higher order harmonics and the total harmonic distortion (THD, defined as the ratio of the square root of the summed squares of the higher order harmonic amplitudes to the amplitude of the fundamental). The THD was typically $\leq$2%, and the phase angle between the stress and strain fundamentals was also calculated. This sequence of equilibrium and dynamic shear tests at 0.15 M NaCl was then repeated sequentially after reequilibration in 0.05, 0.01, 0.5, and 1.0 M NaCl, and corresponding moduli were calculated at each concentration.

Theory

Unit Cell Model. The cylindrical unit cell model of a linear polyelectrolyte surrounded by aqueous electrolyte has been widely used to characterize intermolecular interaction, incorporating the Poisson−Boltzmann equation to calculate the electrical potential and mobile ion distributions[9,15,16] within the unit cell. At a microscopic scale, GAG molecules in cartilage are randomly oriented so that the contribution of electrostatic interactions to the tissue's macroscopic properties can be approximated to be isotropic (often called statistically isotropic[17]) and homogeneous. Moreover, the GAG molecule can be modeled as locally rigid even though its global structure is flexible.[18] Therefore, the average interaction between

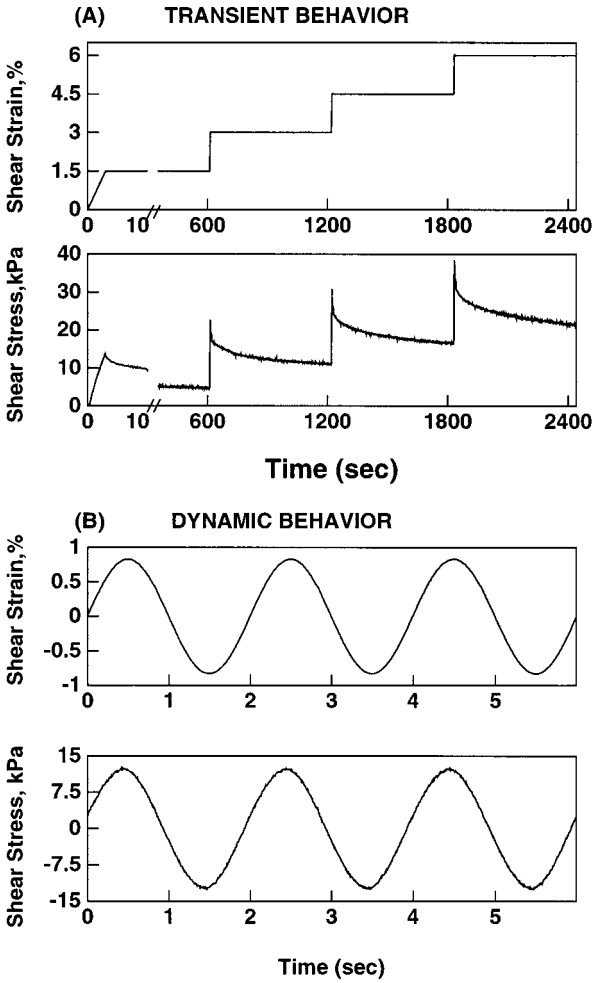

Figure 3. (A) Transient stress−strain tests were used to measure the equilibrium shear modulus. Shear strain was applied as a ramp-and-hold to each final strain increment of 1.5%, causing an initial increase and subsequent relaxation of shear stress by approximately 10 min after application of strain. Initial 10 s of stress and strain data from the first transient are expanded to show the detail. The relaxed stress vs strain values were used to compute the equilibrium shear modulus. (B) Dynamic shear stiffness was assessed by applying a dynamic shear strain of 0.8% amplitude at 0.5 Hz (0% offset shear strain). A discrete Fourier transform (DFT) was performed to calculate the amplitude and phase of the dynamic stress and strain fundamentals and higher order harmonics. Additionally, the total harmonic distortion (THD, see text) was calculated to monitor any distortion in the input (strain) and the response (stress).

neighboring GAG segments was modeled using the PB unit cell, and the GAG segment was approximated as a cylindrical rod having a known surface charge density (Figure 4A). The intercharge distance (b) and the radius (a) of CS-GAG have been reported previously from experimental and structural studies[8,19,20] to be $b = 0.64$ and $a = 0.55$ nm. The unit cell radius, R, is a function of GAG concentration within the tissue:

$$R = \left(\frac{M_{cs}}{2\pi b N C_{GAG}}\right)^{1/2} \quad (1)$$

where N (Avogadro's number) $= 6.02 \times 10^{23}$/mol, $M_{cs} =$ 458 g/mol is the molecular weight of an ionized CS-GAG disaccharide, and C_{GAG} is the GAG concentration in g/m^3. An isotropic compressive deformation, for example, will decrease the unit cell radius (R) by increasing C_{GAG} according to eq 1.

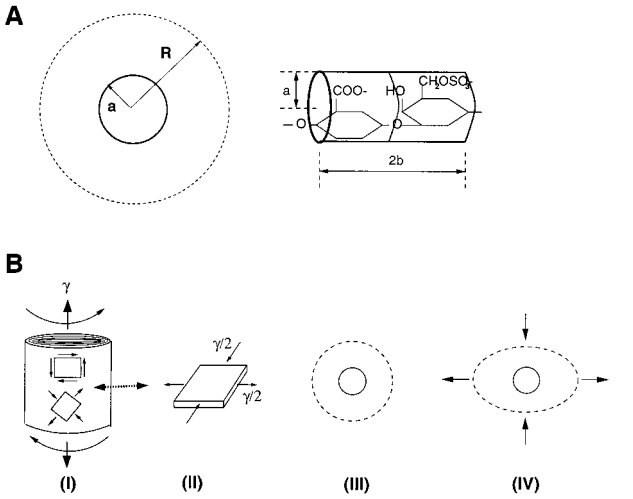

Figure 4. (A) CS-GAG segment was modeled as a charged rod, and its radius (a) and the intercharge distance (b) were set to be 0.55 and 0.64 nm, respectively. The unit cell radius, R, is determined from GAG concentration within the tissue. (B) The effect of the torsional shear deformation (I) on the unit cell within cylindrical tissue is equivalent to that of pure shear deformation (II) on the unit cell within plane stress element, deforming the circular cross section of the unit cell boundary (III) into an ellipsoid (IV).

The effect of torsional shear strain on the unit cell geometry can be approximated to deform the circular cross section to that of an ellipsoid (Figure 4B). For a linear, homogeneous, isotropic material, the shear stiffness of a cylindrical specimen under torsional strain is equal to that of each infinitesimally thin-walled hollow cylinder.[21] The imaginary rectangular element within a thin-walled hollow cylinder (plane stress element) will be subjected to pure shear strain, as pictured in Figure 4B(I). The element will be subjected to pure shear strain, as pictured in Figure 4B(I), which results in a conformational change of the circular boundary of the unit cell ($r = R$) into ellipsoidal one (depending on the orientation of the GAG chain with respect to the plane element), while the circular shape of the GAG surface ($r = a$) maintains its circular geometry (Figure 4B(IV)). For example, the unit cell boundary will experience the maximum of either stretch or compaction when its axis lies along the principal directions of tension/compression. In the present study, we assumed that the probabilistic average of the free energy associated with the conformational change of the randomly oriented unit cell could be obtained from the case in which the unit cell is perpendicular to the plane stress element.[35] The shear modulus of the plane stress element subjected to pure shear strain will be identical to that of the cylindrical material under torsional strain,[17] which allows us to compare the measured shear modulus of the cylindrical specimen to the calculated modulus of the plane stress element. For example, the plane stress element within a hollow cylinder will be subjected to the normal strain $\pm\gamma/2$ along the principal directions of normal stress when the cylindrical specimen is under torsional strain, γ (Figure 4B(II)).[17]

For a linear material under small deformation, the stretch ratio, λ, can be defined in terms of the torsional shear strain γ as

$$\lambda \sim 1 + \frac{\gamma}{2} \tag{2}$$

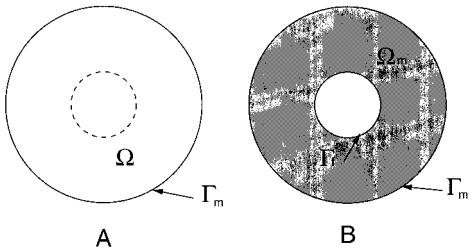

Figure 5. (A) GAG surface (dotted circle) and a unit cell boundary (solid circle). GAG fixed charges are confined within the dotted circle, and mobile ions are confined between the dotted and the solid circles. The PB equation can be represented over the domain (Ω) as $\epsilon_w\nabla^2\Phi = -\rho_f - \rho_m$, and the boundary condition at Γ_m is $\nabla\Phi\cdot\mathbf{n} = 0$, where $\mathbf{n}$ is the outward unit vector normal to the surface. (B) The volume fixed charge density within dotted circle of (A) is replaced by a surface charge density at the GAG surface, Γ_f. The PB equation within domain, Ω_m, can now be expressed as $\epsilon_w\nabla^2\Phi = -\rho_m$, and the boundary condition at Γ_m is $\epsilon_w\nabla\Phi\cdot\mathbf{n} = -\sigma$.

and the reciprocal of the stretch ratio, λ^{-1}, represents the compaction ratio. The deformed unit cell radius becomes $R\lambda$ along the direction of maximum tension and $R\lambda^{-1}$ along the direction of maximum compression. Our objective is to compute the changes in electrical potential and mobile ion distribution within the deformed unit cell of Figure 4B(IV) using the Poisson−Boltzmann theory and to calculate the electrical contribution to the shear modulus from the change in the electrostatic free energy with respect to shear strain.

Poisson−Boltzmann (PB) Equation. The PB equation is based on the Poisson's equation of electrostatics:

$$\nabla\cdot[\epsilon_w(\mathbf{r})\nabla\Phi(\mathbf{r})] + \rho(\mathbf{r}) = 0 \tag{3}$$

and the Boltzmann equation describing the distribution of mobile ions in a dilute electrolyte solution containing only the monovalent ions Na^+ and Cl^-:

$$C_\pm(\mathbf{r}) = C_0 \exp\left(\frac{\mp\mathcal{F}\Phi(\mathbf{r})}{\mathcal{R}T}\right) \tag{4}$$

where C_0 is the concentration of Na^+ and Cl^- ions in bath solution where $\Phi = 0$, $\mathcal{F}$ is the Faraday constant, $\mathcal{R}$ is the gas constant, $\Phi(\mathbf{r})$ is the electrical potential, $\rho(\mathbf{r})$ is the charge density, $\epsilon_w(\mathbf{r})$ is the dielectric permittivity of the solvent, $\mathbf{r}$ is the position vector, and activity coefficients are assumed to be unity. The charge density, ρ, is the sum of the fixed charge ρ_f of the macromolecules and the mobile ions $\rho_m(\mathbf{r}) = \mathcal{F}(C_+(\mathbf{r}) - C_-(\mathbf{r}))$. Insertion of eq 4 into eq 3 gives the form of the Poisson−Boltzmann equation

$$\nabla^2\Phi(\mathbf{r}) = \frac{-\rho}{\epsilon_w} = \frac{-(\rho_f + \rho_m(\mathbf{r}))}{\epsilon_w} = \frac{2\mathcal{F}C_0}{\epsilon_w}\sinh\left(\frac{\mathcal{F}\Phi(\mathbf{r})}{\mathcal{R}T}\right) - \frac{\rho_f}{\epsilon_w} \tag{5}$$

where ϵ_w is assumed to be spatially invariant. In our model, GAG fixed charge is represented by a surface charge density at $r = a$. Therefore, we replace the fixed charge density, ρ_f, with a surface charge density, σ (Figure 5), and the PB equation (eq 5) then takes the form in the fluid phase Ω_m,

$$\nabla^2\Phi(\mathbf{r}) = \frac{2\mathcal{F}C_0}{\epsilon_w}\sinh\left(\frac{\mathcal{F}\Phi(\mathbf{r})}{\mathcal{R}T}\right) \tag{6}$$

We use the notation Γ_m to indicate the outer boundary of the unit cell in the undeformed and deformed state. Henceforth, the PB equation will be considered only in the fluid region, with boundary conditions needed at $r = a$ (Γ_f in Figure 5) and at Γ_m.

Force Equilibrium. In equilibrium, the momentum balance within the fluid phase can be written as[23]

$$0 = \rho_m \mathbf{E} - \nabla P_s \tag{7}$$

where $\mathbf{E}$ is the electric field intensity and P_s is the osmotic swelling pressure defined as

$$P_s = \mathscr{R}\,T\sum_i C_i(\mathbf{r}) = \mathscr{R}\,T(C_+(\mathbf{r}) + C_-(\mathbf{r})) = 2\mathscr{R}\,TC_0\cosh\left(\frac{\mathscr{F}\Phi(\mathbf{r})}{\mathscr{R}\,T}\right) \tag{8}$$

The ith component of eq 7 can then be written as ($\rho_m = \nabla\cdot(\epsilon_w\mathbf{E})$):

$$\left(\frac{\partial\epsilon_w E_j}{\partial x_j}\right)E_i - \frac{\partial P_s}{\partial x_i} = \frac{\partial}{\partial x_j}(T^e_{ij} - \delta_{ij}P) = 0 \tag{9}$$

where the Maxwell stress tensor term, T^e_{ij}, is defined as[24]

$$T^e_{ij} = \epsilon_w E_i E_j - \frac{\epsilon_w}{2}\delta_{ij}E_k E_k \tag{10}$$

Under isotropic compression of the tissue, the components of the electrical field become zero along the unit cell boundary due to the symmetry, leading to $T^e_{ij} = 0$ at Γ_m. Therefore, at this boundary, the osmotic swelling pressure, $P_s(R)$, is the only force balancing the applied external stress. However, the unit cell boundary becomes ellipsoidal in response to a pure shear deformation, inducing a nonzero electric field and a nonzero Maxwell stress tensor component at this boundary. Therefore, we used the energy method to compute the contribution of electrostatic forces to the material shear stress and the shear modulus.

Derivation of Electrostatic Free Energy. The change in the shear modulus with ionic concentration is presumed to be due to the electrical interactions only, so the nonelectrical contribution to the shear modulus, G_{ne}, is assumed to be constant at all ionic concentrations. The electrostatic free energy, $\mathscr{J}$, of the system of Figure 4B is defined as[25]

$$\mathscr{J} = \int_{\Gamma_f}\sigma\Phi\,d\Gamma - \int_{\Omega_m}\left(\Delta\Pi + \frac{\mathbf{E}\cdot\mathbf{D}}{2}\right)d\Omega \tag{11}$$

$$= \int_{\Gamma_f}\sigma\Phi\,d\Gamma - \int_{\Omega_m}\left[2\mathscr{R}\,TC_0\left(\cosh\left(\frac{\mathscr{F}\Phi}{\mathscr{R}\,T}\right) - 1\right) + \frac{\epsilon_w}{2}(\nabla\Phi)^2\right]d\Omega \tag{12}$$

where $\mathbf{D}$ is the electric displacement current density and Π is the osmotic pressure. In eq 11, the first term represents the electrostatic free energy associated with charged GAG surface, the second term corresponds to the osmotic swelling pressure of the unit cell with respect to the reference bath, and the last term represents the electrical stored energy of the fluid phase. We note that eq 11 can also be recast into a form including electrostatic, entropic, and osmotic terms, which is sometimes used as a starting point in this derivation:[25]

$$\mathscr{J} = \int_{\Omega_m}\left(\frac{\mathbf{E}\cdot\mathbf{D}}{2} + T\Delta S - \Delta\Pi\right)d\Omega \tag{13}$$

where ΔS is the entropy change. Using the electrostatic free energy, the electrical contribution to the shear stress, τ_e, induced by the shear deformation can be calculated as

$$\tau_e = \frac{d\mathscr{J}^*}{d\gamma} \tag{14}$$

where γ and $\mathscr{J}^*$ represent shear strain and the electrostatic free energy per unit volume, respectively.

Implementation of the Finite Element Method (FEM) for the PB Equation. An analytical solution of the nonlinear PB equation can only be obtained for the cases of a one-dimensional geometry or a cylindrical geometry in which the fluid contains only counterions.[15] The analytical solution of eq 5 for our case of an ellipsoidal domain does not exist, and therefore the finite element method was used in this study. The implementation of the finite element method is described in detail in the Appendix.

Results

Experiment. After each application of a ramp-and-hold shear strain to final value of 1.5%, the resulting shear stress showed an instantaneous peak stress followed by a stress relaxation behavior (Figure 3A). The equilibrium shear stress recorded after 10−30 min of relaxation increased linearly with applied shear strain at all ionic concentrations (Figure 6A). At each shear strain, the equilibrium shear stress increased monotonically as the ionic concentration decreased. The equilibrium shear modulus, computed by the linear regression from the stress−strain curves, decreased monotonically with increasing NaCl concentration (Figure 6B). The dynamic shear modulus measured at 0.8% strain and 0.5 Hz at each ionic concentration also decreased with increasing NaCl concentration in a similar manner (Figure 6B). The phase angle between the dynamic shear stress and the shear strain decreased monotonically from 18° to 10° with decreasing NaCl concentration.

FEM Implementation. The PB equation was solved over one quadrant of a unit cell using 20 × 20 linear elements having a finer mesh near the cylindrical surface (Figure 7). The normalized electrical potential ($\mathscr{F}\Phi/\mathscr{R}\,T$) was obtained by solving the PB equation, using parameter values for GAG radius $r = 0.55$ nm, the intercharge distance $b = 0.64$ nm from the literature,[9] and a physiological GAG concentration of 6.6% by wet weight ($C_{GAG} = 6\%$ at 0% compression).[26] The theoretical calculation of Figure 7 corresponds to a 6% applied torsional shear deformation reflected on the unit cell at 0.15 M ionic concentration. The electrical potential varied between −51.2 and −15.6 mV, lower near the surface of the GAG chain, and increased quickly away from the surface. The range of the electrical potential shifted to more negative values at lower ionic concentration: −116.2 to −78.8 at 0.01 M, −76.0 to −38.9 at 0.05 M, −32.0 to −2.8 at 0.5 M, and −24.5 to −0.6 mV at 1.0 M. At all ionic concentrations, the

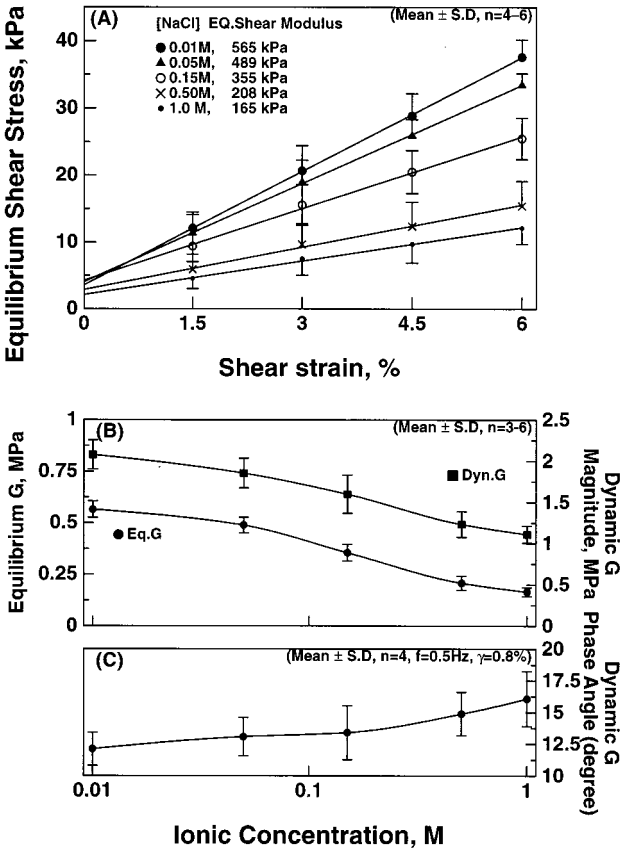

Figure 6. (A) The equilibrium shear stress increased linearly with the applied shear strain. At each strain, the equilibrium shear stress increased monotonically as the ionic concentration decreased. (B) The variation of dynamic shear modulus with ionic concentration was similar to that of equilibrium shear modulus, suggesting the important role of GAG electrostatic interactions in the dynamic properties as well as the equilibrium properties of cartilage in shear. (C) The phase angle between the dynamic shear stress and the applied strain decreased with decreasing ionic concentrations.

potential was more negative near the compressed region along the GAG surface (Figure 7, position b) and the outer boundary of the unit cell (Figure 7, position a). We note that isotropic compressive deformation of cartilage uniformly decreases the outer radius, maintaining a circular shape. Such isotropic compression would therefore not induce any gradient in electrical potential along the GAG and unit cell boundary due to symmetry. In contrast, shear deformation does induce a gradient in potential along the GAG surface from "c" to "d" and the outer boundary from "d" to "a". This is why, in the case of isotropic compression, the swelling pressure at the unit cell boundary is the only force which opposes the applied compression, while there is no corresponding simple relation for the case of shear deformation. Mobile ion distributions in the electrolyte phase were calculated using eq 4 and the computed electrical potential of Figure 7. At 0.15 M bath ionic concentration, the counterion (Na^+) concentration increased above 1.0 M near the GAG surface and the coion (Cl^-) concentration decreased below 0.08 M (Figure 8).

Calculation of Shear Modulus at Different Ionic Concentrations. Shear stress (τ_e) vs shear strain at different ionic concentrations was calculated from eq 14 (Figure 9A). The calculated shear stress was linearly proportional to the shear deformation, similar to the experimental results. At lower ionic concentrations, the increase in the slope saturated more quickly than that in the measurement. At 1.0 M ionic concentration, the calculated equilibrium shear stress changed by only a small amount during 6% shear deformation. The shear modulus of cartilage tissue (G_{total}) can be assumed to be from two parts: the electrical contribution to the shear modulus, G_e, and the ionic strength-independent or nonelectrical contribution to the shear modulus, G_{ne},

$$G_{total} = G_e + G_{ne} \tag{15}$$

Figure 9B shows the comparison of the measured shear modulus (G_{total}) to the calculated electrical contribution to the shear modulus (G_e), using two fitting parameters: the GAG concentration (C_{GAG}) and ionic strength-independent shear modulus (G_{ne}). Using the algorithm referred to as Broyden−Fletcher−Goldfarb−Shanno (BFGS),[27] a variant of conjugate gradient methods, the fitting parameters were determined as $C_{GAG} = 67.7 \pm 4.9$ mg/mL and $G_{ne} = 150.2 \pm 24$ kPa with a 68.3% (±1 standard deviation) confidence level, where the chi-square function (defined as the squared sum of the difference between data and prediction divided by the variances of data) was minimized. To test the goodness-of-fit of the model to the data, we calculated the probability Q that a value of chi-square would be larger than the minimized value by chance due to the variability of the measurement; Q is given by the incomplete gamma function,[27] $Q = \Gamma(N - 2/2, \chi^2/2)$, where N is the number of data points. With the minimized chi-square value, Q was calculated as 0.76; if Q is larger than 0.1, then the goodness-of-fit is said to be believable.[27]

Discussion

The contribution of electrostatic interactions between GAG molecules to the shear stiffness of cartilage was studied by measuring tissue shear modulus under torsional shear deformation at varying ionic concentrations. The observation that the shear modulus of cartilage varies with ionic concentration suggests that electrical interactions do, indeed, contribute to the resistance to shear deformation. In general, such ionic strength-dependent phenomenon could be described over macroscopic length scales by Donnan equilibrium theory or at molecular length scale by the PB equation. However, a charged porous medium subjected to pure shear deformation maintains a constant volume and, hence, constant fixed charge density. Under these conditions, the macroscopic Donnan theory predicts that the Donnan osmotic swelling pressure is unaffected by shear deformation. Therefore, we focused on the molecular-level interactions between GAG molecules represented by the PB theory, and we approximated the GAG as a charged rod within the tissue matrix. The average interaction between segments of GAG molecules under shear deformation was represented as the simultaneous stretch-and-compaction of the unit cell of GAG (Figure 4).

To verify whether this microstructural model of GAG interactions can simulate the experimentally observed dependence of equilibrium shear modulus on ionic strength, we used the nonlinear Poisson−Boltzmann equation and calculated the changes in the electrostatic free energy caused by the deformation and changes in

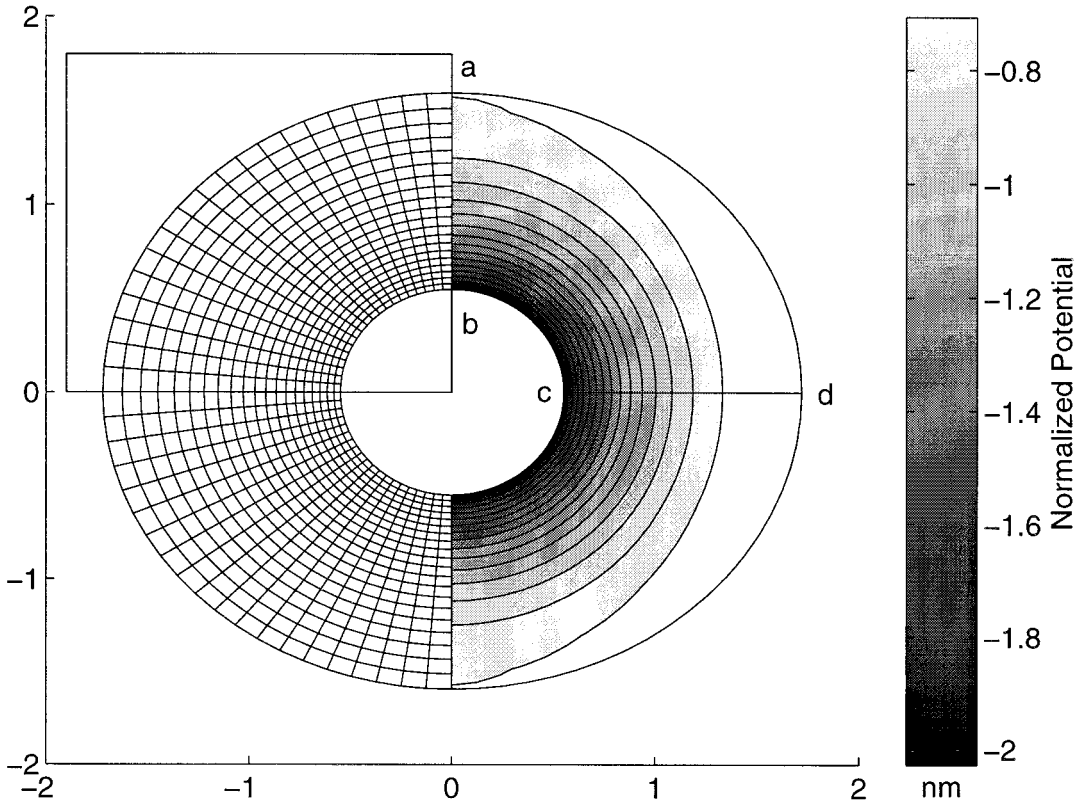

Figure 7. Mesh generation (left half) and the computed electrical potential (right half), $\mathcal{F}\Phi/\mathcal{R}T$, from finite element analyses are shown. The initial conditions were $C_0 = 0.15$ M, $\gamma = 6\%$, and $C_{GAG} = 6.6\%$, the latter corresponding to $C_{GAG} = 6\%$ at 0% compression. 400 (20 by 20) elements were generated in one quadrant of the unit cell (within a box), and finer meshes were allocated near the GAG surface.

ionic strength. The electrical contribution to the equilibrium shear stress, τ_e, was calculated as a function of shear strain and ionic strength using the energy method, and the electrical contribution to the equilibrium shear modulus, G_e, was obtained from the slope of the stress−strain curve. The predicted equilibrium shear modulus agreed well with measurement using the fitted parameter values of $C_{GAG} = 6.77\%$ and $G_{ne} = 150$ kPa. The measured GAG concentration in new-born calf femoropatellar groove cartilage has been reported previously to be $5.6 \pm 0.6\%$ by wet weight.[26] Considering the measurement here was performed at 10% compressive offset strain, the predicted value of C_{GAG} is physiologically reasonable. The best fit value of G_{ne} was found to be 150 kPa, which is close to the value obtained by extrapolating the measured equilibrium shear modulus above 1.0 M concentration (Figure 3B). In addition, the equilibrium shear modulus of cartilage measured after enzymatic extraction of GAG was found independently to be in the range between 100 and 150 kPa.[28]

The variation of dynamic shear modulus with ionic concentration was similar to that of the equilibrium shear modulus. This observation implies that electrostatic interactions between GAGs are also important determinants of the dynamic shear modulus of cartilage. Furthermore, the decrease in phase angle between dynamic shear stress and strain toward zero degrees upon decreasing the ionic concentration shows the importance of elastic restoring forces that are inherent to electrostatic interactions. It is interesting to note that the dynamic shear modulus of our cartilage specimens decreased with decreasing frequency. In a separate set of experiments (data not shown), we observed that the amplitude of the dynamic shear modulus reduced to that of the equilibrium shear modulus at frequencies below 0.0001 Hz, which was measured at 0.15 M bath ionic concentration.

The dynamic shear and compressive modulus of cartilage have been reported previously by us and others to be dependent on frequency.[11,29] This has most often been attributed to (1) the intrinsic viscoelastic properties of the matrix macromolecules and (2) the frictional interaction between fluid and solid phases, e.g., the poroelastic deformations associated with fluid flow through the water-filled matrix. Both such effects cause the dynamic modulus to be greater than the equilibrium modulus by an amount that varies with frequency. In this study we have used torsional shear deformation applied to the tissue as a whole where, for low deformation amplitude, the motions are essentially volume conserving. As a result, torsional tissue shear deformation involves little or no macroscopic fluid flow with respect to the solid network. (Both fluid and solid elements deform together.) Thus, the measured frequency dependence of the shear modulus in our experiments is likely due to the intrinsic viscoelastic properties of macromolecular network of collagen and proteoglycans. For the case of volumetric (e.g., compressive) deformation, which can induce significant levels of fluid flow, both fluid−solid (poroelastic) interactions and ionic strength-dependent viscous effects including the electroviscous effect may also be important.[29,30]

The electrical potential obtained by solving the PB equation shifted to more negative values with decreasing ionic concentration. As the bath ionic concentration decreases, there will be less counterions available to

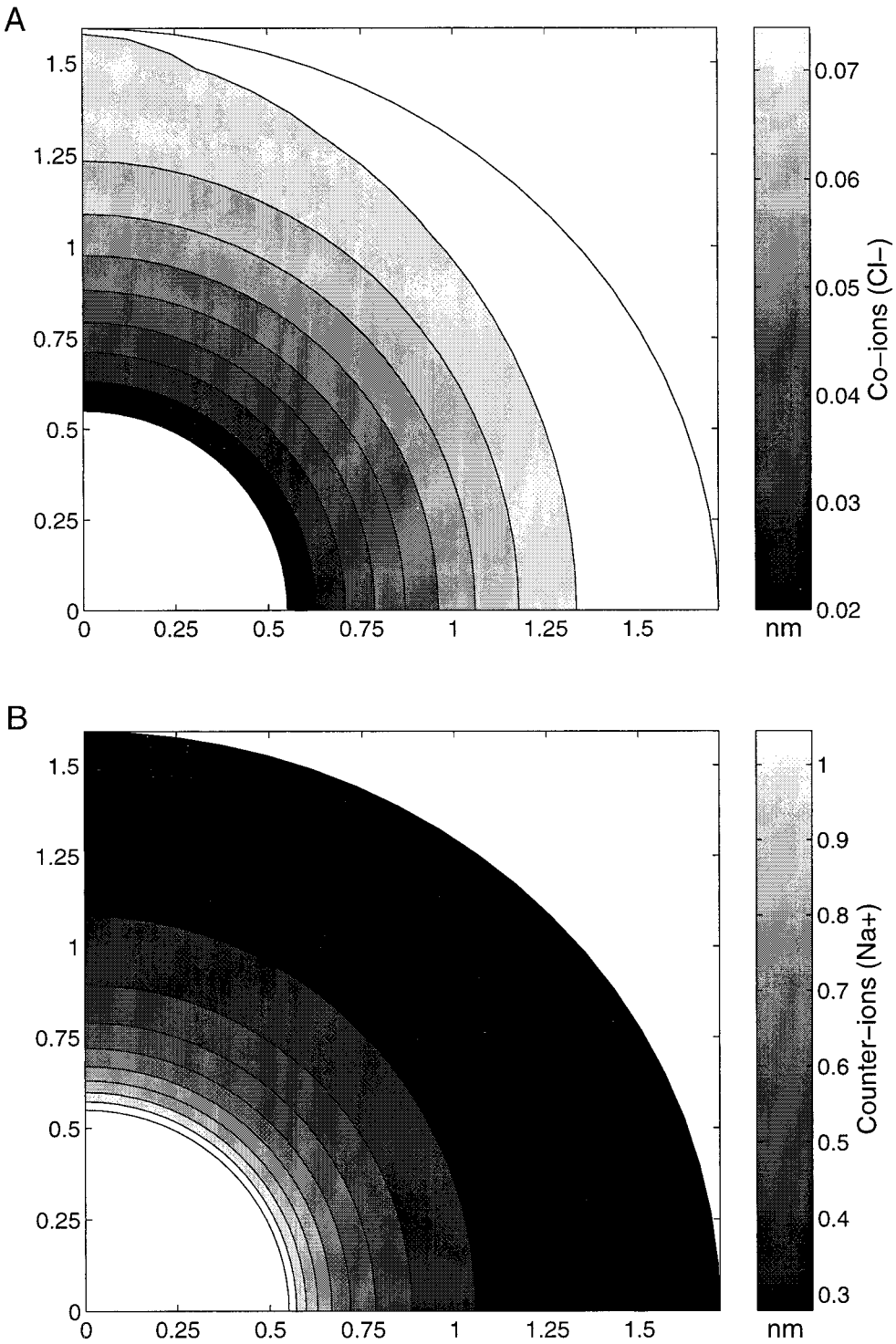

Figure 8. Concentrations of co- and counterions were calculated using the Boltzmann equation (eq 4) and the computed electrical potential obtained in Figure 7.

shield the negative charges of GAG. However, at higher ionic concentration, the electrical repulsion will be shielded so that further shear deformation no longer increases the repulsive force. This shielding effect results in the saturation of the measured shear properties at higher ionic concentration (Figure 6), which is also apparent in the theoretically predicted shear behavior at 1.0 M ionic strength (Figure 9).

In this study, the electrostatic free energy was obtained using the method of Sharp and Honig.[25] This free energy includes the chemical charging energy associated with GAG fixed charge and the electrical and osmotic energy of the mobile ion phases (e.g., eq 11). These terms can be recast into the electrostatic, entropic, and osmotic terms. The validity of this definition of the electrostatic free energy was independently tested for our system for the case of isotropic compression of the unit cell, by comparing the macroscopic stress calculated using the energy method to the direct calculation of the total swelling pressure evaluated at the unit cell boundary. The two different calculations gave essentially same result.

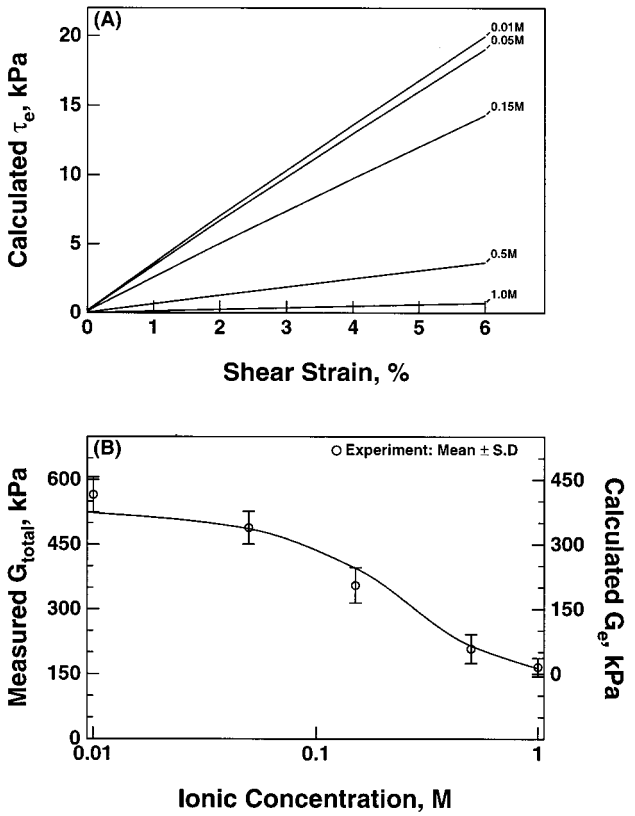

Figure 9. (A) Electrical contribution to the equilibrium shear stress (τ_e) was calculated from eq 14. The following parameter values were used for this calculation: $a = 0.55$ nm, $b = 0.64$ nm, $C_{GAG} = 6.6\%$, and $C_0 = 0.15$ M. (B) Data represent the measured shear modulus, determined from the stress vs strain slopes of Figure 6A, as shown in Figure 6B. The electrical contribution to shear modulus (G_e) was computed with two fitting parameters, C_{GAG} and G_{ne}. C_{GAG} and G_{ne} were determined to be 67.7 ± 4.9 mg/mL and 150.2 ± 24 kPa, respectively, at which the chi-square value was minimized.

The contributions of electrical and nonelectrical interaction to the volumetric compressive deformation of cartilage have been described previously.[9,31] The nonelectrical contribution to the compressive stiffness can be ascribed to the structural rigidity and elasticity of matrix macromolecules, steric interactions, and the entropic effect of the change in the number of possible configurations of the GAG chains and other molecules. This latter entropic term is called "entropic elasticity"[6] under compressive deformation. Under physiological ionic strength conditions, the entropic contribution of GAG molecules to the compressive stiffness was estimated theoretically to be ~10%.[31] However, under volume-conserving shear deformation, the contribution of this entropic effect to the equilibrium shear modulus will be minimal. Therefore, nonelectrical contributions to the shear modulus are more likely associated with the elastic properties of collagen fibrillar network and other resident macromolecules and, possibly, steric interactions at the molecular level.

In summary, the electrostatic interactions between GAG molecules, immobilized within 3-D tissue network subjected to shear deformation, have been modeled using the PB unit cell model. The numerical FEM solution of the PB equation allows the calculation of the change in the electrostatic free energy due to shear or isotropic compressive deformations and combinations of these deformations. Further extensions of this constitutive model will be useful for describing the details of nonelectrical or ionic strength-independent contributions to the shear modulus.

Acknowledgment. This research was supported by NIH Grant AR33236.

Appendix

The integral formulation of the PB equation is

$$\int \tilde{\Phi}(\nabla^2\Phi - f(\Phi))\, d\Omega_m = 0 \tag{16}$$

where $f(\Phi) = (2\mathcal{F}C_0/\epsilon_w)\sinh(\mathcal{F}\Phi/\mathcal{R}T)$ and $\tilde{\Phi}$ is virtual electrical potential. The appropriate boundary conditions for the integral formulation are

$$\Gamma_f: \nabla\Phi\cdot\mathbf{n} = -\frac{\sigma}{\epsilon_w} \quad \Gamma_m: \nabla\Phi\cdot\mathbf{n} = 0$$
$$\Gamma_f \cup \Gamma_m = \Gamma \quad \Gamma_f \cap \Gamma_m = 0 \tag{17}$$

where $\mathbf{n}$ is the outward unit vector normal to surface, Γ_f and Γ_m. The variational form of eq 16 can be obtained by applying Green's theorem,

$$\int \tilde{\Phi}\mathbf{n}\cdot\nabla\Phi\, d\Gamma_f - \int (\nabla\tilde{\Phi}\nabla\Phi + \tilde{\Phi}f(\Phi))\, d\Omega_m = 0 \tag{18}$$

The same shape function, $P(r,s)$, is assumed for the potential and the space (isoparametric FEM), which is defined in a curvilinear coordinate (r,s),

$$\Phi = [P]\{\hat{\Phi}\} \quad \tilde{\Phi} = [P]\{\hat{\tilde{\Phi}}\}$$
$$X = [P]\{\hat{X}\} \quad Y = [P]\{\hat{Y}\} \tag{19}$$

where $(\wedge)$ represents the nodal value. For a linear 4-node rectangular element, $P(r,s)$ becomes

$$P(r,s) = \frac{1}{4}[(1+r)(1+s)\,(1-r)(1+s)\,(1-r)(1-s)\,(1+r)(1-s)] \tag{20}$$

Equation 18 becomes the matrix equation for all the nodal values, $\hat{\Phi}$, as unknown variables,[32]

$$[A][\hat{\Phi}] + [B(\hat{\Phi})] + [C] = [0] \tag{21}$$

where

$$A_{ij} = \int_{-1}^{1}\int_{-1}^{1}\left(\frac{\partial P_i}{\partial X}\frac{\partial P_j}{\partial X} + \frac{\partial P_i}{\partial Y}\frac{\partial P_j}{\partial Y}\right)\det J\, dr\, ds$$

$$B_i = \int_{-1}^{1}\int_{-1}^{1} P_i f(\Phi)\det J\, dr\, ds$$

$$C_i = \int_{-1}^{1} P_i\frac{\sigma}{\epsilon}\Delta_1\, dr + \int_{-1}^{1} P_i\frac{\sigma}{\epsilon}\Delta_2\, ds + \int_{-1}^{1} P_i\frac{\sigma}{\epsilon}\Delta_3\, dr + \int_{-1}^{1} P_i\frac{\sigma}{\epsilon}\Delta_4\, ds$$

$$\Delta_1 = \left[\left(\sum_{i=1}\frac{\partial P_i}{\partial r}X_i\right)^2 + \left(\sum_{i=1}\frac{\partial P_i}{\partial r}Y_i\right)^2\right]^{1/2} \quad \text{along } s = -1$$

$$\Delta_2 = \left[\left(\sum_{i=1}\frac{\partial P_i}{\partial s}X_i\right)^2 + \left(\sum_{i=1}\frac{\partial P_i}{\partial s}Y_i\right)^2\right]^{1/2} \quad \text{along } r = 1$$

$$\Delta_3 = \left[\left(\sum_{i=1} \frac{\partial P_i}{\partial r} X_i\right)^2 + \left(\sum_{i=1} \frac{\partial P_i}{\partial r} Y_i\right)^2\right]^{1/2} \quad \text{along } s = 1$$

$$\Delta_4 = \left[\left(\sum_{i=1} \frac{\partial P_i}{\partial s} X_i\right)^2 + \left(\sum_{i=1} \frac{\partial P_i}{\partial s} Y_i\right)^2\right]^{1/2} \quad \text{along } r = -1$$

and J is a Jacobian matrix, $\partial(X,Y)/\partial(r,s)$.

Because of the nonlinearity, eq 21 is solved through an iterative scheme. Let a nonlinear operator F be defined as

$$[F(\hat{\Phi})] = [A][\hat{\Phi}] + [B(\hat{\Phi})] + [C] \tag{22}$$

Then the differential of F is expressed as

$$[\Delta F(\hat{\Phi})] = [A] + [\Delta B(\hat{\Phi})] \tag{23}$$

Using Newton's method for the iteration scheme,

$$[\Delta F(\hat{\Phi})]_n[\Delta \hat{\Phi}]_{n+1} = -[F(\hat{\Phi})]_n \tag{24}$$

and the potential is updated as

$$[\hat{\Phi}]_{n+1} = [\hat{\Phi}]_n + [\Delta \hat{\Phi}]_{n+1} \tag{25}$$

where subscript n means the nth iteration. The stopping criterion for the iteration was when the change in $\hat{\Phi}$ was less than 0.1% for every nodal value. Because of symmetry, one quadrant of the unit cell was digitized as 20 × 20 elements (within the box in Figure 7).

References and Notes

(1) Wight, T. N.; Heinegard, D. K.; Hascall, V. C. In *Cell Biology of Extracellular Matrix*, 2nd ed.; Plenum Press: New York, 1991.
(2) Grodzinsky, A. J.; Levenston, M. L.; Jin, M.; Frank, E. H. *Annu. Rev. Biomed. Eng.* **2000**, *2*, 691−713.
(3) Lander, A. D.; Selleck, S. B. *J. Cell. Biol.* **2000**, *148*, 227−232.
(4) Ripamonti, A.; Roveri, N.; Braga, D. *Biopolymers* **1980**, *19*, 965−975.
(5) Bowes, J. H.; Kenton, R. H. *Biochem. J.* **1948**, *43*, 358−365.
(6) Anand, L. *Comput. Mechanics* **1996**, *18*, 339−355.
(7) Honig, B.; Sharp, K.; Yang, A.-S. *J. Phys. Chem.* **1993**, *97*, 1101−1109.
(8) Comper, S. D.; Laurent, T. C. *Physiol. Rev.* **1978**, *58*, 255−315.
(9) Buschmann, M. D.; Grodzinsky, A. J. *J. Biomech. Eng.* **1995**, *117*, 179−192.
(10) Lai, W. M.; Hou, J. S.; Mow, V. C. *J. Biomech. Eng.* **1991**, *113*, 245−258.
(11) Zhu, W.; Mow, V. C.; Koob, T. J.; Eyre, D. R. *J. Orthop. Res.* **1993**, *11*, 771−781.
(12) Basser, P. J.; Schneiderman, R.; Bank, R. A.; Wachtel, E.; Maroudas, A. *Arch. Biochem. Biophys.* **1998**, *351*, 207−219.
(13) Bursac, P.; McGrath, C. V.; Eisenberg, S. R.; Stamenovic, D. *J. Biomech. Eng.* **2000**, *122*, 347−353.
(14) Frank, E. H.; Jin, M.; Loening, A.; Levenston, M. L.; Grodzinsky, A. J. *J. Biomech.* **2000**, *33*, 1523−1527.
(15) Katchalsky, A. *Pure Appl. Chem.* **1971**, *26*, 327−373.
(16) Einevoll, G.; Hemmer, P. C. *J. Chem. Phys.* **1988**, *89*, 474−482.
(17) Crandall, S. H.; Dahl, N. C.; Lardner, T. H. In *An Introduction to the Mechanics of Solids*, 2nd ed.; McGraw-Hill: New York, 1978.
(18) de Gennes, P. G. *Colston Papers No. 29. Ions in Macromolecular and Biological Systems.* In Scientechnica, Bristol, UK, 1978; pp 69−79.
(19) Preston, B. N.; Snowden, J. M.; Houghton, K. T. *Biopolymers* **1972**, *11*, 1645−1659.
(20) Ogsten, A. G.; Preston, B. N.; Wells, J. D. *Proc. R. Soc. London* **1973**, *333*, 297−316.
(21) The measurement of compressive properties of cartilage has shown linearity between stress and strain under small deformation.[22] This linearity was also observed in our measurement of shear stress vs strain for up to 6% strain.
(22) Eisenberg, S.; Grodzinsky, A. J. *J. Orthop. Res.* **1985**, *3*, 148−159.
(23) Sanfeld, A. In *Introduction to the Thermodynamics of Charged and Polarized Layers;* John Wiley & Sons: New York, 1967.
(24) Melcher, J. R. In *Continuum Electromechanics*; MIT Press: Cambridge, MA, 1981.
(25) Sharp, K.; Honig, B. *J. Phys. Chem.* **1990**, *94*, 7684−7692.
(26) Sah, R. L.; Kim, Y.-J.; Doong, J. H.; Grodzinsky, A. J.; Plaas, A. H. K.; Sandy, J. D. *J. Orthop. Res.* **1989**, *7*, 619−636.
(27) Press: W. H.; Flannery, B. P.; Teukolsky, S. A.; Vetterling, W. T. In *Numerical Recipes*; Cambridge University Press: New York, 1986.
(28) Personal communication with P. Bursac.[13]
(29) Frank, E. H.; Grodzinsky, A. J. *J. Biomech.* **1987**, *20*, 615−627.
(30) Allison, S. A. *Macromolecules* **1998**, *31*, 4464−4474.
(31) Kovach, I. S. *Biophys. Chem.* **1996**, *59*, 61−73.
(32) James, A. E.; Williams, D. J. A. *J. Colloid Interface* **1985**, *107*, 44−59.
(33) Buckwalter, J. A.; Poole, A. R.; Reiner, A.; Rosenberg, L. C. *J. Biol. Chem.* **1982**, *257*, 10529−10532.
(34) Hardingham, T.; Bayliss, M. *Semin. Arthritis. Rheum.* **1990**, *20* (3 Suppl 1), 12−33.
(35) The change in free energy was also calculated[36] using detailed probabilistic averaging over all GAG orientations using the method of Quinn.[37] The result using this further refined method gave $C_{GAG} = 54.3$ mg/mL (which is even closer to the measued value) and $G_{ne} = 161$ kPa (which is within 10% of the present model).
(36) Jin, M. Ph.D. Thesis, MIT, 2001.
(37) Quinn, T. M.; Dierickx, P.; Grodzinsky, A. J. *J. Biomech.* **2001**, in press; Quinn, T. M. Ph.D. Thesis, MIT, 1996.

MA0106604